Rare Metal Materials and Engineering
Volume 46, Issue 6, June 2017
Online English edition of the Chinese language journal

Available online at www.sciencedirect.com
ScienceDirect

Cite this article as: Rare Metal Materials and Engineering, 2017, 46(6): 1491-1496.

ARTICLE

Burst Test Research on Zirconium Alloy for Nuclear Fuel Cladding Tubes

Zhang Yanwei, Wang Rongshan, Bai Guanghai, Liu Erwei, Mei Jinna

Suzhou Nuclear Power Research Institute, Suzhou 215004, China

Abstract: To evaluate the mechanical properties and promote a better understanding of failure behavior of the newly developed Zr-Nb cladding tubes during reactivity initiated accidents (RIAs), burst tests were carried out with the biaxial stress state under different pressurization rates at the temperature ranging from 293 to 623 K. The influence of pressurization rate and test temperature was characterized in this test. The pressurization rates were 0.97 GPa/s at 293 K, 0.62 GPa/s at 473 K, and 0.49 GPa/s at 623 K for the fast pressurization test, and 0.23 MPs/s for the ASTM burst test. Maximum hoop stress was increased by 10.61%, 9.32% and 8.26% compared to the ASTM burst test at 293, 473 and 623 K, respectively. The results show that the burst ultimate hoop stresses (UHS) at rupture decrease while the total circumferential elongation (TCE) increased monotonically with the rise of temperature, the uniform circumferential elongation (UCE) is not significantly affect by the test temperature. All the burst tests result in ductile ballooning failure, and cracks initiate and propagate along the axial direction above the maximum hoop stress. A higher pressurization rate leads to shorter but wider cracks. As the test temperature is raised, the ductility increases and the propagation of the axial crack is suppressed.

Key words: Zr alloy; burst testing; cladding; pressurization rate; temperature

There are a number of significant researches on the confirmation of fuel safety in commercial light water reactors (LWR) under accident conditions. Reactivity-initiated accident (RIA) is one of the most important design-based accidents in LWR. When a RIA occurs in LWR, a rapid increase in power with the width over 100 ms[1] leads to nearly adiabatic heating of the fuel pellets, which deform by a thermal expansion and a release of the gaseous fission product was caused by the opening of a grain boundary in the fuel pellet. In case the pellet clad gap is narrow or closed, which normally happens with cladding degraded as the burn-up proceeds, pellet clad mechanical interaction (PCMI) will lead to rapid and biaxial mechanical loading of cladding tube and the cladding failure can be induced[2].

Our understanding of the fuel behavior during RIA is based on the results of RIA simulation tests, which performed on instrumented short-length fuel rod in dedicated test reactors, and on the results of separated effect tests, which are carried out on fuel or cladding samples out of pile. These tests consist of tube burst, axial tension, and ring tension. The main facilities where relevant RIA tests have been generated were built in the Japanese NSRR test reactor[3], the French CABRI reactor[4], and the Russian BIGR reactors[5]. The reactor tests are done at conditions that approximate those expected in power reactors under RIA, and they provide valuable information on the integral fuel rod behavior under the accident. However, these tests cost much and it is also difficult to do further investigation due to the irradiation-induced radioactivity. Out of pile tests, performed under well controlled conditions, are therefore used to study the deformation and fracture behavior of a fuel cladding under RIA conditions.

Fundamental to these tests is that cladding failure occurs by fracture due to hoop expansion; so many tests have evolved to determine the mechanical properties of cladding

Received date: June 14, 2016
Corresponding author: Zhang Yanwei, Ph. D., Life Management Technology Center, Suzhou Nuclear Power Research Institute, Suzhou 215004, P. R. China, Tel: 0086-512-68702413, E-mail: zhangyanwei2010@cgnpc.com.cn

samples tested in the hoop direction. These tests consist of ring tensile test, tube burst, expansion due to compression (EDC) test, ring compression test, plane-strain tensile test and the magneto-forming test[6]. In these test methods, the ring tension test is widely used because of the small specimen size and the easiness of the experimental procedure. Considering the characteristic of RIA (the ratio of the circumferential to the axial stress $\sigma_{zz}/\sigma_{\theta\theta}$ is 0.5), a plane-strain transverse tensile test was developed[7] and then adapted by PROMETRA program[8]. Burst test is also extensive by used pressure-controlled loading test with the biaxial stress state at the ratio $\sigma_{zz}/\sigma_{\theta\theta}=0.5$. Usually the burst tests are pressure ramps with constant increase of pressure rates. A conventional burst test was usually performed according to the ASTM B811 specification with pressure increasing rate of 0.23 MPa/s. Recently, a rapid burst test was suggested to promote a better understanding of failure behavior of PWR fuel rods during RIAs[9]. The effect of hydride accumulations on Zircaloy-4 claddings mechanical properties was investigated[3]. A similar rapid pressurization burst test was also performed on HANA-4 cladding[10]. Burst test of Zr-1Nb cladding was also performed under the pressure increasing rate of 1~2 MPa/s[11]. So far, there is few burst test results of Zr-1Nb tubes which wereperformed at high pressurization rate ~ 1 GPa/s in the literature. The objective of this study is to investigate the mechanical behavior of a newly developed Zr-1Nb alloy cladding under a rapid pressurization to simulate a RIA condition. The effect of the test temperature and the pressure increase rate were also analyzed, which must be considered at the design of the advanced cladding for a high burn-up operation.

1 Experiment

1.1 Burst test

Fig.1 shows a schematic illustration of the burst test equipment (IVS-G3011-A-200). Cladding sample (16) was fixed to the holder at upper end, while lower end (15) of sample was free for axial movement, which can be also loaded with requirement. Resistance heating furnace (13) with accuracy grade ±3 was installed around a quartz tube with the test specimen in side. It gave a 300 mm length heating zone with the max temperature of 773 K. Non-flammable silicon oil (ISO viscosity grade of 43) was used as the pressurization medium for all the tests. The oil is extensively low compressive and it has very low viscosity. The equipment can be used for the burst test under pressurization rate ranging from 0.01 MPa/s to 1 GPa/s. In order to investigate the influence of test temperature, all specimens were tested at room temperature (293 K), 473 and 623 K.

Before the fast pressurization (FP) burst test starts, the GB-30 accumulator gas booster (6) was boosted by the low pressure pump (3) and high pressure pump (4) to 206.9 MPa (30000 psi). After that, the unloading valve (9) between the accumulator gas booster (6) and the cladding specimen (16) immediately was released so that it led to a cladding failure in a short time. Pressure profile was measured by a pressure sensor (11) under the sampling frequency of 400 kHz. Over 80 000 data points were collected within 1 s into the main memory all at once during the test, and then they are saved in the hard disk drive computer after the test. Heating furnace (13) which can be heated up to 673 K was used around the test specimen. Zr-1Nb cladding was tested at room temperature (293 K), 473 and 623 K. Non-flammable silicon oil (Shinetsu KF-96) was used in the study as the pressurization medium.

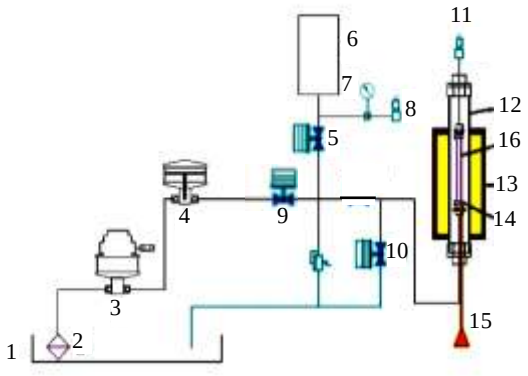

1, 2, 3, 4, 6: high-pressure system; 5, 9, 10: some control valves; 7, 8, 11: pressure sensors; 12,13: heating furnace; 14,15: sample holders; 16: cladding sample

Fig.1 Schematic illustration of the burst test equipment

Besides the FP burst test, a conventional burst test was also performed according to the ASTM B811 specification with pressure increasing rate of 0.23 MPa/s. When the ASTM burst test started, the low pressure pump (3) pushed the high pressure pump (4) to boost the cladding specimen (16) with pressure increasing rate of 0.23 ±0.1 MPa/s.

In both FP burst and ASTM burst test, the end part of cladding was tightly constrained so that the biaxiality of the test specimen was accurately controlled to be 2. The burst UHS were calculated using the thin-wall formula:

$$\sigma_\theta=pD/2t$$

where p is internal pressure, D is the mean diameter (average of OD and ID) and t is the thickness of the tube.

1.2 Test specimen

The studied Zr-1Nb alloy was developed by the Suzhou Nuclear Power Research Institute (SNPI). The Zr-1Nb alloy tubes for tests were taken from a domestic manufacturer, and the production is still in trial stage. The forging temperature was 1303 K and the final annealing temperature of the claddings was 883 K. The microstructure was assumed to be

an aging recrystallization state. The specimens were cut from the finished tube directly, the external diameter was 9.5 mm and the wall thickness was 0.57 mm. The chemical composition with respect to the alloying elements is described in Table 1. The length of specimens was 150 mm. After the test, the total circumferential elongation (TCE) and the uniform circumferential elongation (UCE) were determined by measuring the fracture area and the average several points away from the fracture area, respectively.

2 Results and Discussion

2.1 Microstructure of the as-received tubes

Fig.2 shows the microstructures of the tested tube. Zirconium alloys have different microstructure with the effect of annealing and chemical composition. Annealing induces microstructural changes such as recrystallization and grain growth, which affect the mechanical properties. A high strength is achieved when the alloys are cold-worked or further annealed at low temperatures. On the other hand, the ductility and elongation would be good under a high temperature annealing which results in recrystallized microstructures. For Zr-Nb alloys, because of the eutectoid reaction, the final annealing is usually performed at a lower temperature of 883 K.

Recrystallized zirconium alloys are suitable for nuclear applications because of their low irradiation growth, and high irradiation creep resistance. According to Fig.2, the final microstructure of the annealed Zr-1Nb alloy was shown to be the equiaxed grain with the grain sizes of 3~7 μm, which was assumed to be an annealing recrystallization state.

2.2 Burst behavior

As for the ASTM burst tests at various temperatures, the pressure increased smoothly with the increasing rate of ~14 MPa/min, which were about 0.23 MPa/s according to the ASTM B811 specification. The burst pressure was 84.8, 62.2 and 46.0 MPa at 293, 473, and 623 K, respectively, while the corresponding UHS was 664.27, 487.23 and 360.33 MPa. The actual duration time (ADT) of the fuel cladding in FP test was 339.73, 248.63 and 180.86 s.

Fig.3 shows the time–pressure curves of Zr-1Nb tubes under the FP burst test. All the three curves are a similar in shape. It shows a low invariable pressure primarily because it takes some time to transfer the pressure to the specimen through the accumulator. After a short detention, a fast linear increase of pressure is observed before the cladding yielded. The pressure increases or decreases at the range of 10 MPa for over 100 ms until the cladding failure. The

Table 1 Chemical composition of the tested Zr-1Nb tube (wt%)

Nb	Cu	O	N	H	Zr
1.11	0.01	0.12	0.006	0.002	Bal.

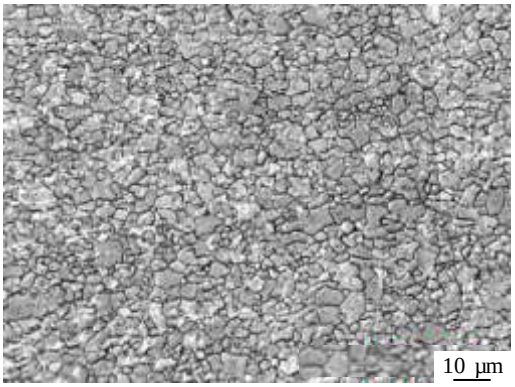

Fig.2 Microstructure of the tested Zr-1Nb tube

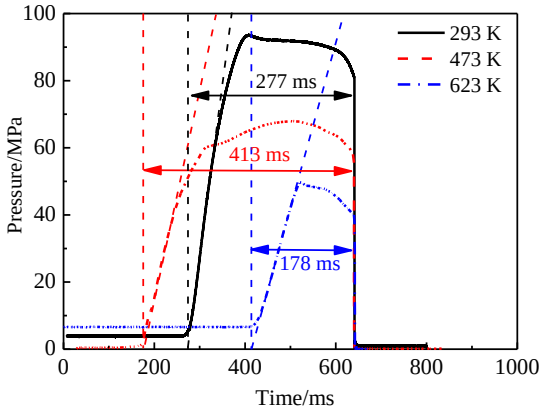

Fig.3 Pressure-time curves of Zr-1Nb tubes under the FP burst test

pressure increasing rate was estimated by calculating the slope of the initial linear part of time-pressure curve. In this study, the pressure increasing rate of FP burst were 0.97 GPa/s at 293 K, 0.62 GPa/s at 473 K, and 0.49 GPa/s at 623 K, where the pressurization rate at 293K temperature is 4347 times faster than that of the ASTM burst test. Compared to the ASTM burst test, the mechanical properties change in FP burst due to the fast pressurization. The burst pressure was 93.6, 68.0 and 49.8 MPa at 293, 473, and 623K, respectively, which mean the UHS at 293, 473, and 623 K were 733.20, 532.67 and 390.10 MPa, respectively, increased by 10.38%, 9.32% and 8.26%, respectively.

When estimating the ADT of the fuel cladding in FP test, a line was drawn from the elastic region and extended to the baseline. The intersection point was suggested to be the starting point and the point at a failure was suggested to be the final point. In this study, the ADT of the Zr-1Nb cladding was 277, 413 and 178 ms at 293, 473, and 623 K, respectively, which approximates to the power pulse of an actual RIA situation, namely around 20~200 ms[3]. It is clear that the test pressure decreases after the yield point at

both 293 and 623 K while kept on increasing until another yield point, which cause the longer ADT at 473 K than others.

Post-test examination of specimens was performed after the tests. As shown in Fig. 4, all the specimens performed a ductile rupture, creating a circumferentially ballooned state. With the maximum hoop stress created by the inter-pressure of tubes, crack initiated and extended along the axial direction. After that, cracks performed various in morphology according to the test conditions. They could be classified into three types. In the case of FP burst test at 293 K, the crack stopped extending along the axial direction after a period, and then teared along the hoop direction because of the hoop stress and rapid pressurization, creating a creak along the hoop direction. The tube tested at 293 K performed the largest strength. In the case of ASTM burst test at 293, 473 K and FP burst test at 473, 623 K, sharp cracks became blunt during a plastic deformation and then stopped to extend. In the case of ASTM burst test at 623 K, it is obvious that the shape of the end part of the ballooned region was dull when compared to other specimens. It indicated that the ductility was increased to suppress the extension of the axial crack at an elevated temperature, which corresponded to the lowest strength. When comparing the ASTM and FP burst test at 293 and 473 K, it is clear that a higher pressurization rate results in a shorter but wider crack. As the test temperature increased, the crack got wider. The crack was apparently wider at 623 and 473 K than that at 293 K under the condition for both ASTM and FP burst tests. Similar situation was also reported at Zr-4 tubes under the rapid pressurization[10].

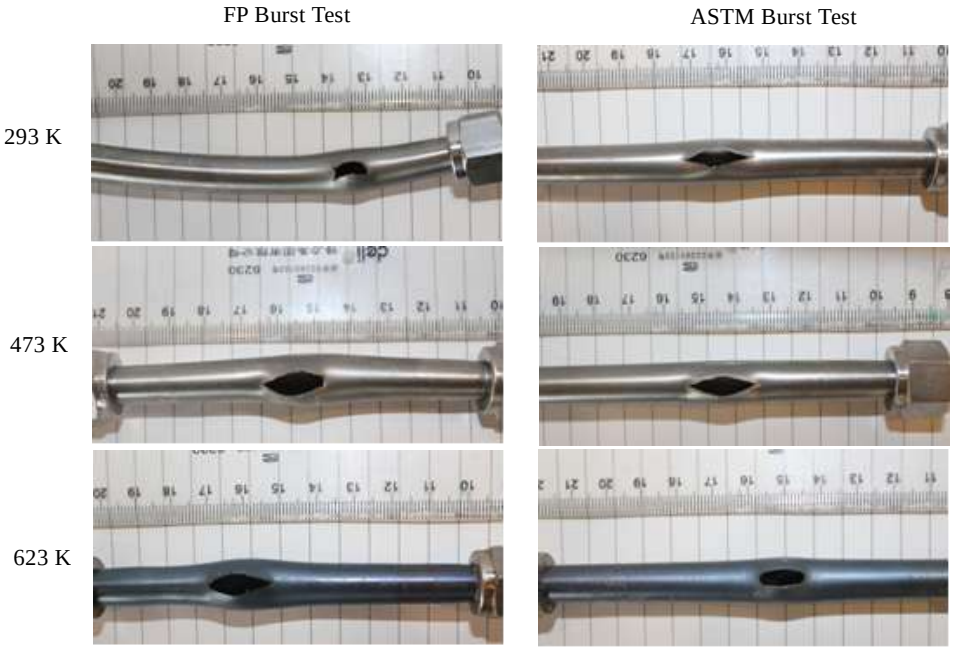

Fig.4 Appearance of Zr-1Nb cladding specimens versus pressurization rate and temperature

2.3 Effect of pressurization rate

The burst properties of Zr-1Nb tubes at various temperatures were listed, gathering all burst tests into a single graph, and the variability of the material mechanical property as UHS with the pressurization rate is shown in Fig. 5. The burst properties of Zr-1Nb tubes at various temperatures under the rate of 1 MPa/s are also listed in Fig.5. The UHS increased monotonically with the pressurization rate increased. It should be noticed that the UHS of specimens at 423 K under the rate of 1 MPa/s was listed without fitting the data at 473 K. It was suggested that a higher pressurization rate induced a higher strain rate which resulted in the increase of the UHS[11]. In this study, such a strain rate hardening was also observed. Since the evaluation of the actual strain rate under biaxial burst is

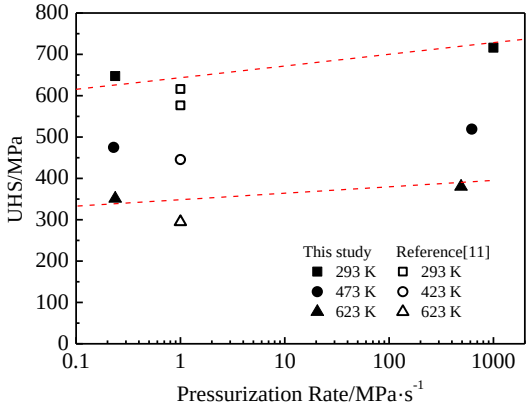

Fig. 5 Changes in the maximum hoop stress of Zr-1Nb with the pressurization rate and the test temperature

extremely difficult, it is tried to evaluate the strain rate of the cladding indirectly.

2.4 Effect of test temperature

Fig.6 shows the correlation of the UHS versus temperature. The UHS at rupture decreased monotonically with the increasing of temperature. The UHS of FP burst test was higher than that of the ASTM burst test, which was explained to be the strain rate hardening. However, this effect is reduced significantly as the temperature rises. The UHS of specimens under the rate of 1 MPa/s also presented the same tendency, but it was lower than that of ASTM burst test. That might be due to the variability of the mechanical properties of the test Zr-1Nb tubes. The general data trend within the temperature range from 293 to 623 K agrees with the data previously obtained within the temperature range from 973 to 1473 K[11]. It proves the correctness of both the experimental and analytical procedures used, and it also proves the absence of additionally significant physical effects on the cladding behavior.

The TCE and UCE of the specimens are plotted in Fig. 7 as functions of temperature. They were used to characterize the ductility of the Zr-1Nb tubes. It shows a tendency that the TEC increases with the rise of temperature. For FP burst test with a high pressurization rate, the TCE increases from 25.95 to 31.69% with the rise of temperature, while for ASTM burst test with a low pressurization rate, the TCE are 10.28, 19.95, and 24.49% at 293, 473, and 623 K, respectively. The slope between the TEC and temperature was 0.0174 for FP test and 0.0434 for ASTM test. It suggested that a higher temperature results in a larger TCE while a higher pressurization rate results in a lower change of TCE. Post-test examination results in Fig. 4 also confirm that the balloon of ASTM test at 293 K was obscured when compared with other specimens, while the crack was the longest, which indicated the worst ductility.

TCE of the ring test is much easier to obtain, and it gives a slightly increasing tendency with the rise of temperature in the range of 293 to 723 K[11]. It is suggested that characterizing the TCE was various because of the different

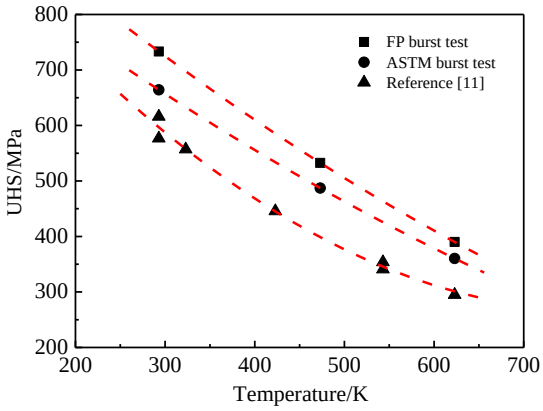

Fig. 6 Correlation of the UHS versus temperature

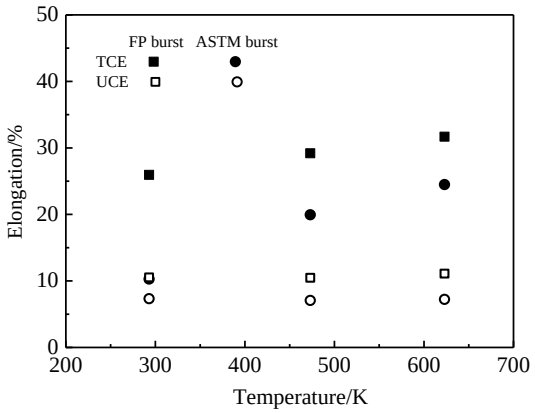

Fig.7 Changes in TCE and UCE of Zr-1Nb tubes with temperature

methods of calculation. The tube specimens along axial direction also exhibited the same tendency although anisotropy of the specimens took place in this temperature zone. The analysis of the UCE shows that the effect of test temperature was very weak, while the effect of the pressurization rate was significant. The UCE of FP burst test was ~10.5% but UCE of ASTM burst test was ~7%.

TCE of the burst test was monotonically increased with the increase of temperature, while UCE was stabilized with the increase of temperature. It indicated that all the test specimens performed ductile under the test condition. Residual hoop strain, which is also used to characterize the ductility of cladding tubes, was reported to be affected by hydrogen absorption. During the waterside corrosion, the generated hydrogen is partly absorbed into the cladding. When hydrogen content exceeds significantly the solubility limit, the hydrides precipitate. These precipitations of the hydrides have a deleterious impact on the fuel cladding ductility. In this study, fresh tubes were tested without the precipitation of the hydrides. The effect of hydrogen absorption will be investigated in the future.

3 Conclusions

1) Maximum hoop stress are 733.20, 532.67 and 390.10 MPa, at 293, 473, and 623 K, respectively, increased by 10.61%, 9.32% and 8.26% when compared to the ASTM burst test results.

2) Failure mode for the burst test is a ductile ballooning. Crack initiate and propagate along the axial direction above the maximum hoop stress. A higher pressurization rate results in a shorter but wider crack. As the test temperature increases, the ductility increases and the propagation of the axial crack is suppressed.

3) The UHS at rupture decreases monotonically while the TCE increases monotonically with the rise of temperature. The UCE was not significantly affected by the test temperature.

References

1 Luxat J C, Novog D R. *Nuclear Engineering and Design*[J], 2011, 241: 590

2 Fuketa T, Nagase F, Sugiyama T. *IAEA Technical Meeting on Fuel Behavior Modeling under Normal, Transient and Accident Conditions and High Burnups*[C]. Kendal, United Kingdom: IAEA, 2005: 58

3 Nagase F, Fuketa T. *Journal of Nuclear Science and Technology*[J], 2005, 42: 58

4 Papin J, Cazalis B, Frizonnet J M *et al*. *Nuclear Technology*[J], 2007, 157: 230

5 Vitanza C. *Nuclear Engineering and Technology*[J], 2007, 39: 591

6 Desquines J, Koss D A, Motta A T *et al*. *Journal of Nuclear Materials*[J], 2011, 412: 250

7 Link T M, Koss D A, Motta A T. *Nuclear Engineering and Design*[J], 1998, 186: 379

8 Cazalis B, Bernaudat C, Yvon P *et al*. *Proceedings of 18th International Conference on Structural Mechanics in Reactor Technology, SMiRT 18-C02-1*[C]. Beijing: SMiRT, 2005: 383

9 Electric Power Research Institute. *Failure Behavior of PWR Fuel Rods during RIAs*, TR-1003405[R], 2004

10 Kim J H, Lee M H, Jeong Y H *et al*. *Nuclear Engineering and Design*[J], 2008, 238: 1441

11 Kaplar E *et al*. *International Agreement Report*, NUREG/IA-0199 IPSN 01-16[R], 2012

燃料包壳锆合金的爆破性能

张晏玮，王荣山，柏广海，刘二伟，梅金娜

(苏州热工研究院有限公司，江苏 苏州 215004)

摘　要：模拟了燃料包壳用 Zr-Nb 合金管材在 RIA事故工况下的失效行为，研究了温度和升压速率对管材爆破性能的影响。不同温度下快速爆破时的升压速率分别为 293 K 时 0.97 GPa/s，473 K时0.62 GPa/s，623 K 时 0.49 GPa/s；参考 ASTM 标准实施的爆破试验在各温度下的升压速率均为 0.23 MPa/s。结果表明，爆破温度升高，管材爆破强度降低，破口的环向延伸率升高，管材的均匀延伸率受温度影响不明显。所有测试条件下管材均呈鼓包失效，破口沿轴向延伸，升压速率高，破口更宽。温度越高，管材塑性增加，破口长度减小。

关键词：包壳材料；爆破测试；升压速率；温度

作者简介：张晏玮，男，1984 年生，博士，苏州热工研究院有限公司寿命管理技术中心，江苏 苏州 215004，电话：0512-68701169，E-mail: zhangyanwei2010@cgnpc.com.cn